

Analysis of the polarization characteristics of scattered light of underwater suspended particles based on Mie theory*

CHENG Qian (程谦), WANG Ying-min (王英民)**, and ZHANG Ying-luo (张莹珞)

School of Marine Science and Technology, Northwestern Polytechnical University, Xi'an 710000, China

(Received 2 March 2020; Revised 18 April 2020)

©Tianjin University of Technology 2021

Aiming at the problem of underwater polarized laser scattering caused by underwater suspended particles, the equivalent spherical particle Mie scattering theory simulation method is used to study the polarization characteristics of underwater scattered light. The relationship between underwater suspended particle characteristics and optical characteristics is analyzed, and the effects of particle size, polarization characteristics of incident light, and angle of incidence on the degree of polarization of forward and backward scattering light are studied. The results show that: When the incident light is natural light, the degree of polarization of scattered light is very low at the forward-scattering angle, which increases with the increase of the scattering angle, but changes frequently with the increase of the particle size. When the incident light is linearly polarized, the degree of linear polarization of the scattered light is related to the azimuth Angle. The degree of circular polarization is largely unaffected by particle size.

Document code: A **Article ID:** 1673-1905(2021)04-0252-5

DOI <https://doi.org/10.1007/s11801-021-0039-0>

In recent years, underwater polarization imaging has become a hot topic in the field of underwater optical imaging. For underwater optical imaging, the strong scattering and absorption of light by seawater media is a technical bottleneck that limits its development^[1-5]. Since the wavelength of light is comparable to the size of suspended particles and organic molecules in seawater, the scattering of light is far more serious than the scattering of acoustic waves in seawater and causes the degradation of imaging quality. Polarization imaging technology uses the inherent parameter of light wave polarization to properly screen the polarization state of light, filter out scattered photons from the medium, and retain the imaging photons of the target. Thereby the contrast and resolution of the imaging will be improved. Therefore, the research on the polarization characteristics of the scattered light of underwater suspended particles is of great significance to the application of polarization imaging technology.

In 1963, Duntley S Q and Gilbert G D et al studied the transmission characteristics of light waves in the ocean and found a transmittance window^[4] similar to that in the atmosphere. In this window, the attenuation of blue and green light in the 470 nm—583 nm band by seawater is much smaller than that of other light bands^[5,6]. This window band becomes an ideal underwater light source. Since the constituents of underwater

environments are widely varied, there have been various underwater scattering models. For the convenience of study, underwater suspended particles can be usually assumed to be spherical. Since the radius of equivalent spherical particles in water is greater than the wavelength of incident light, the underwater scattering model can be equivalent to the Mie scattering model^[7-9]. There have been several underwater optics studies based on the Mie scattering theory in recent years^[10-12]. This article uses Mie scattering theory to establish a single scattering model of a single underwater scattering particle. By studying the polarization characteristics of forward and backward scattered light of a single underwater suspended particle, the polarization characteristics of scattered photons with different scattering angles are analyzed, and the types of polarized light sources suitable for underwater polarization imaging are studied. At the same time, the polarization characteristics of the backscattering noise of the particles are analyzed to provide a theoretical basis for the noise reduction and restoration algorithms of underwater polarization imaging.

In this analysis, the impurity particles underwater are assumed to be single spherical particles. The scattering model is shown in Fig.1. In Fig.1, I_0 is the incident light, θ is the scattering angle, β is the azimuth of the scattered light, and r denotes the particle radius.

* This work has been supported by the National Natural Science Foundation of China (No.61404362).

** E-mail: ywang@nwpu.edu.cn

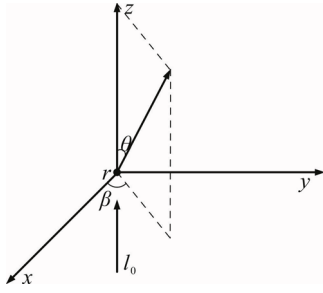


Fig.1 The scattering model

When the plane wave hits a single spherical particle, according to Mie theory, Eq.(1) presents the scattering matrix on the basis of the single-scattering theory:

$$S_i = \begin{bmatrix} S_1(\alpha, \theta) & 0 \\ 0 & S_2(\alpha, \theta) \end{bmatrix}, \quad (1)$$

where S_1 and S_2 are the scattering functions of scattering angle θ and represent the vertical and parallel components of the complex amplitude function of the scattered light respectively; they are infinite series. $\alpha=2\pi r/\lambda$ represents the particle size parameter. The expressions of S_1 and S_2 are as follows:

$$\begin{cases} S_1(\alpha, \theta) = \sum_{n=1}^{\infty} \frac{2n+1}{n(n+1)} (a_n \pi_n + b_n \tau_n) \\ S_2(\alpha, \theta) = \sum_{n=1}^{\infty} \frac{2n+1}{n(n+1)} (b_n \pi_n + a_n \tau_n) \end{cases}, \quad (2)$$

where n is number of term in series. π_n and τ_n indicate the scattering angle coefficient.

$$\begin{cases} \pi_n = \frac{P_n^{(1)}(\cos \theta)}{\sin \theta} \\ \tau_n = \frac{d}{d\theta} P_n^{(1)}(\cos \theta) \end{cases}, \quad (3)$$

where $P_n^{(1)}(\cos \theta)$ is the first order n class of Legendre functions, and a_n and b_n refers to the Mie scattering coefficient:

$$\begin{cases} a_n = \frac{\psi_n(\alpha)\psi_n'(m\alpha) - m \cdot \psi_n'(\alpha)\psi_n(m\alpha)}{\xi_n(\alpha)\psi_n'(m\alpha) - m \cdot \xi_n'(\alpha)\psi_n(m\alpha)} \\ b_n = \frac{m \cdot \psi_n(\alpha)\psi_n'(m\alpha) - \psi_n'(\alpha)\psi_n(m\alpha)}{m \cdot \xi_n(\alpha)\psi_n'(m\alpha) - \xi_n'(\alpha)\psi_n(m\alpha)} \end{cases}, \quad (4)$$

where $\psi_n(\alpha) = \sqrt{\frac{\alpha\pi}{2}} J_{n+\frac{1}{2}}(\alpha)$, $\xi_n(\alpha) = \sqrt{\frac{\alpha\pi}{2}} H_{n+\frac{1}{2}}^{(2)}(\alpha)$,

$J_{n+\frac{1}{2}}(\alpha)$ and $H_{n+\frac{1}{2}}^{(2)}(\alpha)$ are the Bessel function of the first kind and Hankel function of the second kind respectively; ψ' and ξ_n' are their differential. m stands for the complex refractive index of the particle, and $m=m_1-im_2$, where m_1 and m_2 indicates the real and imaginary parts respectively; the real part represents light scattering by particles, and the imaginary part refers to the absorption of light by particles. When the imaginary part is 0, the particles have no absorption to light.

The scattering and extinction cross sections are respectively expressed as

$$\begin{cases} \sigma_{sca} = \frac{\lambda^2}{2\pi} \sum_{n=1}^{\infty} (2n+1) (|a_n|^2 + |b_n|^2) \\ \sigma_{ext} = \frac{\lambda^2}{2\pi} \sum_{n=1}^{\infty} (2n+1) \text{Re}(a_n + b_n) \end{cases}. \quad (5)$$

The scattering and extinction efficiency factors are the ratios of scattering and extinction cross-sections to the spherical particle geometric cross-section, respectively, and are expressed as $Q_{sca}=\sigma_{sca}/(\pi r^2)$, $Q_{ext}=\sigma_{ext}/(\pi r^2)$.

This paper mainly analyzes the influence of particles on the polarization characteristics of the scattered light, so only a single particle size distribution is considered. Therefore, on the basis of the Mie scattering theory of spherical particles, the scattering and extinction coefficients are respectively:

$$\begin{cases} b(\lambda) = N\pi r^2 Q_{sca} \\ c(\lambda) = N\pi r^2 Q_{ext} \end{cases}, \quad (6)$$

where N is the number of particles per volume. The absorption coefficient is $a(\lambda)=c(\lambda)-b(\lambda)$. The single-scattering albedo $\omega=b/c$ is also an important parameter to analyze laser transmission characteristics, and is defined as the percentage of scattering loss in the total attenuation loss.

The complete polarization state can be expressed by the Stokes vector $S=[I, Q, U, V]^T$, where I is the total light intensity, Q and U represent linearly polarized lights in two directions, and V denotes the circularly polarized light. The degree of polarization (*DOP*)

$DOP = \sqrt{Q^2 + U^2 + V^2}/I$ is used to describe the polarization state of the laser. $DOP=1$ indicates a completely polarized light, $DOP=0$ represents a natural light, $0 < DOP < 1$ signifies a partially polarized light,

$DOPL = \sqrt{Q^2 + U^2}/I$ is the linear polarization, and $DOCP = V/I$ denotes the degree of circular polarization (*DOCP*)^[13,14].

Suppose the Stokes vector of the incident photon is $S_0=[I_0, Q_0, U_0, V_0]^T$, then the expression of Stokes vector S after one scattering events in seawater by photon transmission is as follows:

$$S = A(-\beta)M(\theta)A(\beta)S_0, \quad (7)$$

where θ is the photon scattering angle and M stands for the photon Mueller matrix. The expression is as follows:

$$M(\theta) = \begin{bmatrix} m_{11}(\theta) & m_{12}(\theta) & 0 & 0 \\ m_{12}(\theta) & m_{11}(\theta) & 0 & 0 \\ 0 & 0 & m_{33}(\theta) & m_{34}(\theta) \\ 0 & 0 & -m_{34}(\theta) & m_{33}(\theta) \end{bmatrix},$$

$$m_{11} = \frac{1}{2} (|S_1|^2 + |S_2|^2), \quad m_{12} = \frac{1}{2} (|S_1|^2 - |S_2|^2),$$

$$m_{33} = \frac{1}{2} (S_1 S_2^* + S_2 S_1^*), \quad m_{34} = \frac{i}{2} (S_1 S_2^* - S_2 S_1^*), \quad (8)$$

where A represents the scattering rotation matrix:

$$A(\beta) = \begin{bmatrix} 1 & 0 & 0 & 0 \\ 0 & \cos(2\beta) & \sin(2\beta) & 0 \\ 0 & -\sin(2\beta) & \cos(2\beta) & 0 \\ 0 & 0 & 0 & 1 \end{bmatrix}, \quad (9)$$

and β denotes the angle that Stokes vectors of incident light are rotated from the reference surface to the scattering surface.

In the simulation test, the particle radius is selected as 0.6—5 μm , the number of particles per volume is $N=10^9$

and 532 nm green light is selected for simulation. The suspended particles in seawater are mainly algae plankton and sand sediment. On the basis of Tab.1, the real part range of algae particles' complex refractive index is between 1.15 and 1.18, and the imaginary part range is between 0.045 and 0.07. However, the real part of sand sediment particles' complex refractive index ranges from 1.5 to 1.53, and the imaginary part range is between 10^{-4} and 10^{-3} [15,16]. Therefore, $m=1.53-0.001i$ and $m=1.18-0.07i$ were used to simulate the polarization states of scattered light with different incident light types and different scattering angles.

Firstly, natural light is used as incident light to simulate in Mie scattering environment. Fig.2 shows that the *DOP* is not only related to the scattering angle, but also has a great relationship with the particle size. With the increase of particle size, the distribution of the polarization degree of the overall scattered light changes frequently with the scattering Angle, and the larger the particle size, the higher the frequency of the change. In general, the overall scattered light has a lower *DOP* at the forward-scattering angle and a higher *DOP* at the backscattering angle, and the *DOP* of forward-scattering slightly increases with the increase of the particle radius.

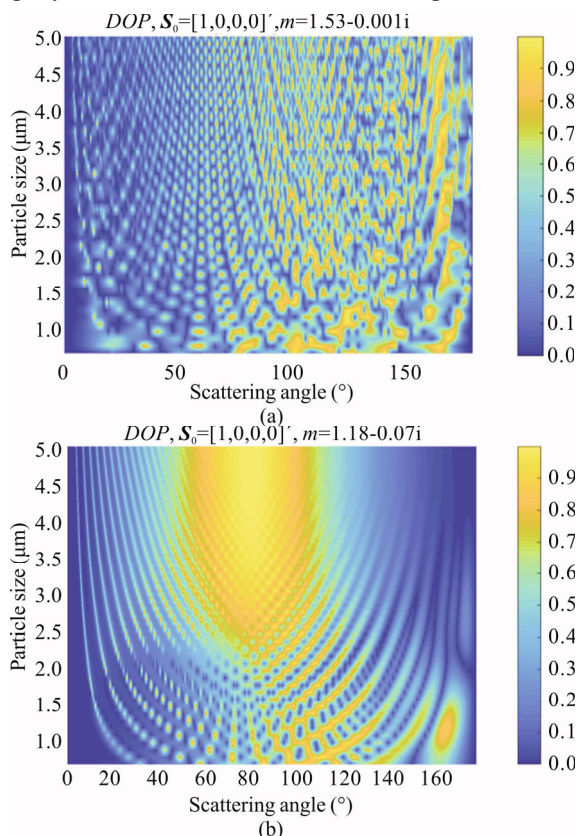


Fig.2 The scattering polarization distribution of natural light, where 0° is the incident direction

Secondly, the linearly polarized light is taken as the incident light, and the result is shown in Fig.3. The particle radius is 0.6 μm in Fig.3(a) and (b), and that is 5 μm in Fig.3(c). It can be seen that the *DOLP* of linearly polarized is not only related to the scattering angle, but also has a relationship with the azimuth. Both forward-scattering and backscattering have a good polarization-preserving ability.

Compared with the case of natural light, no matter at any azimuth Angle, the forward-scattering light has a higher *DOLP* when the incident light is linearly polarized. It's just the opposite of the case of natural light incident. At azimuth 0°, 90° and 180°, the change of *DOLP* with scattering Angle is not sensitive. The *DOLP* at other azimuth angles varies with the scattering Angle, especially in the backscattering. As the particle size increases, the *DOLP* changes more frequently with the scattering angle. When the particle size is large, the polarization distribution exhibits a fine-striped structure, but around the azimuth angles of 0°, 90°, and 180°, the polarization degree is still insensitive to changes in the scattering angle, and it can be considered that it is independent of the azimuth angle. From the perspective of scattering, the *DOLP* of backscattered light decreases with the increase of particle size.

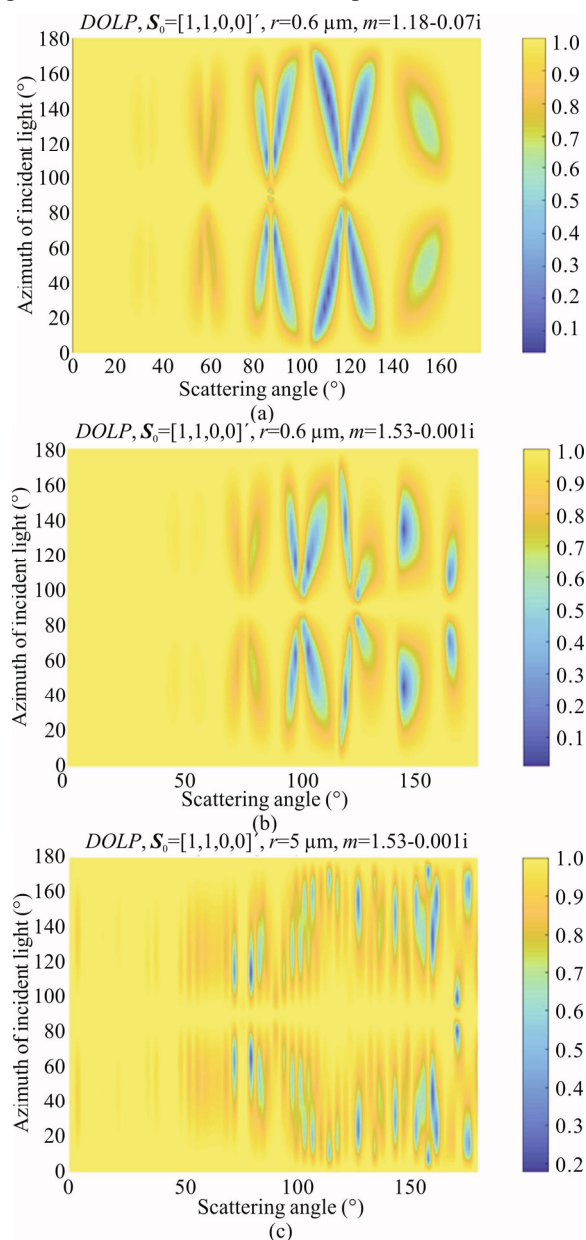


Fig.3 The scattering polarization distribution of linearly polarized light with azimuth variation, where 0° is the incident direction

Considering that the azimuth angle in actual situations is generally fixed and the particle radius may change continuously, three azimuth angles: 15°, 30°, and 60° are selected as the representative for simulation to analyze the variation of the polarization degree of scattered light with the particle size and scattering angle. Fig.4(a)—(c) in turn gives the distribution of the overall scattered light polarization degree at these three azimuth angles. It can be seen from the figure that the overall scattered light has a high degree of polarization at the forward scattering angle, close to linearly polarized light. However, the polarization degree distribution at the backscatter angle changes frequently, and has little relationship with the change of particle radius, but it changes significantly with the azimuth angle.

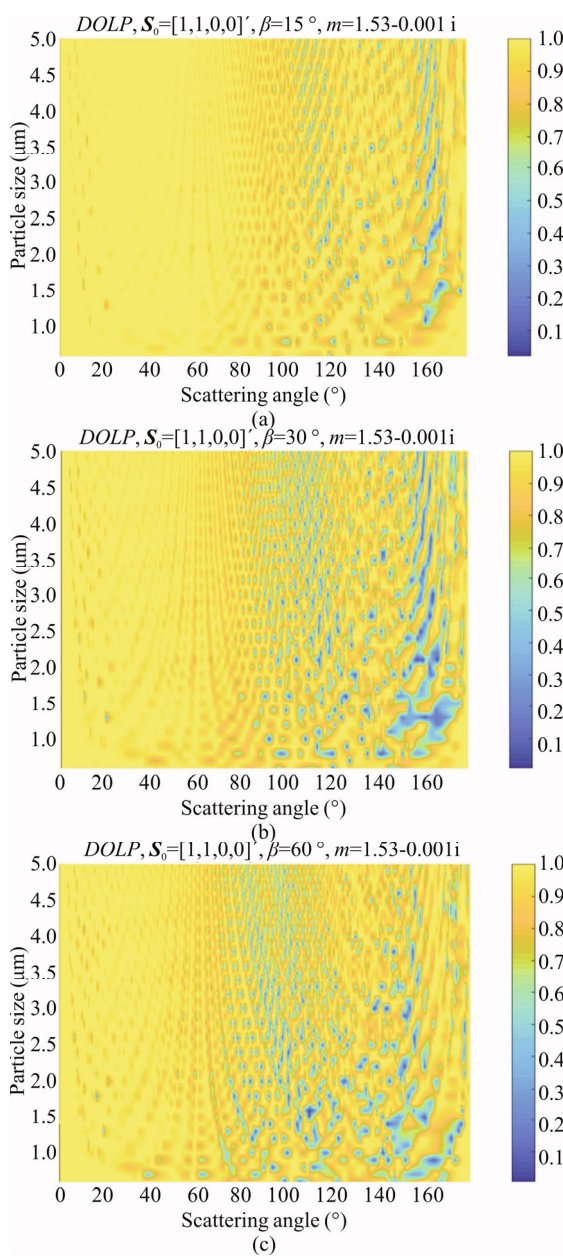


Fig.4 The scattering polarization distribution of linearly polarized light, where 0° is the incident direction

Finally, the right-handed circularly polarized light and the left-handed circularly polarized light were used as the incident light source for simulation. The simulation results are shown in Fig.4. It can be seen from Fig.4(a) and (b) that as the particle size increases, *DOCP* changes more frequently with the change of the scattering angle, but this change mainly occurs in the side scattering, while the forward scattering and the back scattering the backscattered *DOCP* is basically unchanged. By comparing Fig.4(b) and (c), it can be seen that either left-handed or right-handed circularly polarized light is used as the incident light source, the backscattering is different from the rotation polarity of the incident light, that is, the backscattered circularly polarized light has the

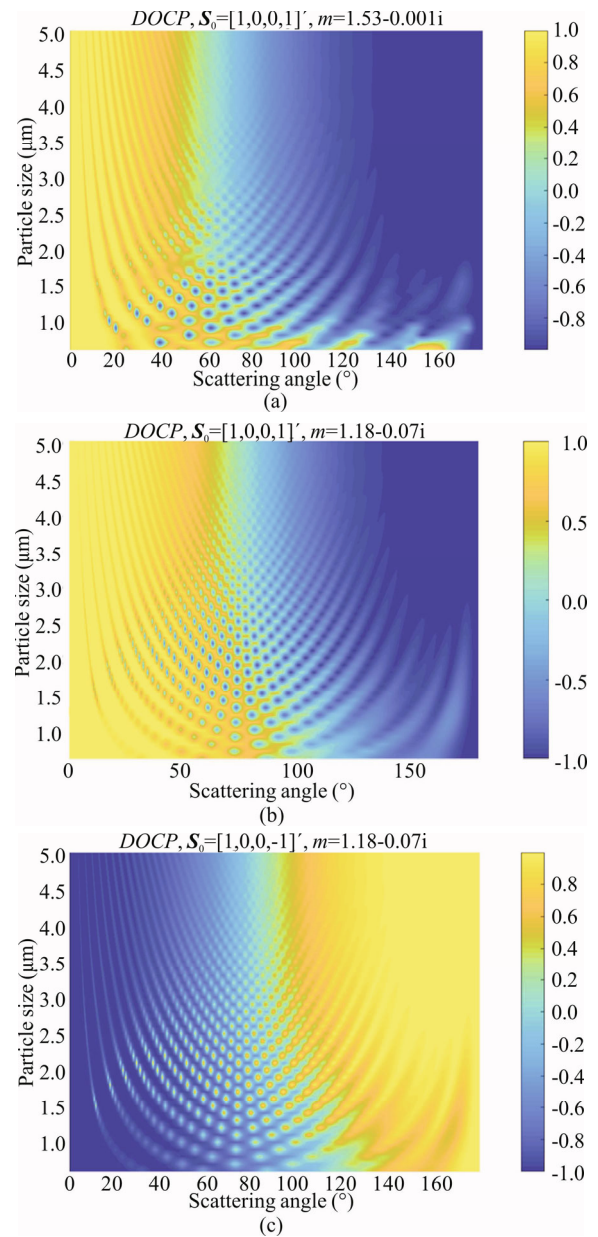


Fig.5 The scattering polarization distribution of circularly polarized light, where 0° is the incident direction

opposite direction, but it is still circularly polarized in nature, so forward scattering and backscatter both have good polarization retention. Compared with linearly polarized light, circularly polarized light has a stronger polarization maintaining ability.

In this study, an underwater photon's scattering is simulated on the basis of a method combining Mie scattering theory. This paper has comprehensively analyzed the effect of suspended particles on the underwater polarized light polarization characteristics. The research shows: When the incident light is natural light, most of the scattered light is partially polarized light. The *DOP* of scattered light is very low at the forward-scattering angle, which increases with the increase of the scattering angle, but changes frequently with the increase of the particle size. When the incident light is linearly polarized, the *DOLP* of the scattered light is related to the azimuth angle. The *DOLP* of forward-scattering and backscattering is very high, and only when the azimuth angle is far away from 0° , 90° and 180° will there be a small *DOLP* and it also changes frequently with the increase of particle size. When circularly polarized light is used as the incident light, both the forward-scattering and the backscatter polarization are high, but the polarization rotation of the backscattered light is reversed. The *DOCP* is largely unaffected by particle size. Therefore, when using underwater polarization imaging technology, an active circularly polarized light source can be used to improve the quality of received image.

References

- [1] G. Zaccanti, P. Brusaglioni, M. Gurioli and P. Sansoni, *Applied Optics* **32**, 1590 (1993).
- [2] S. Zhang, J. T. Zhan, S. K. Bai, Q. Fu, J. Duan and H. L. Jiang, *Acta Optica Sinica* **36**, 0729001 (2016). (in Chinese)
- [3] O. K. Steinvall, *Proceedings of SPIE - The International Society for Optical Engineering* **32**, 1307 (1992).
- [4] H. H. He, N. Zeng, R. Liao and H. Ma, *Progress in Biochemistry and Biophysics* **42**, 419 (2015). (in Chinese)
- [5] R. M. Lerner and J. D. Summers, *Applied Optics* **21**, 861 (1982).
- [6] Q. Duntley, *Journal of the Optical Society of America* **53**, 214 (1963).
- [7] G. C. Wang, S. F. Dong, D. Wen and M. Qiao, *Electronic Technology* **47**, 68 (2010). (in Chinese)
- [8] K. Ding, Y. W. Huang, W. Q. Jin, K. J. Jin and H. L. Li, *Infrared Technology* **35**, 467 (2013). (in Chinese)
- [9] J. E. Hansen, *Journal of Atmospheric Sciences* **28**, 120 (1971).
- [10] J. E. Hansen and L. D. Travis, *Space Science Reviews* **16**, 527 (1974).
- [11] I. W. Sudiarta and P. Chylek, *Journal of the Optical Society of America A* **18**, 1275 (2001).
- [12] L. Ma, F. Duan, G. Song and L. Zhao, *Measurement* **117**, 125 (2018).
- [13] A. Ishimaru, S. Jaruwatanadilok and Y. Kuga, *Applied Optics* **40**, 5495 (2001).
- [14] P. Sun, Y. Ma, W. Liu, C. Xu and X. Sun, *Journal of Optics* **15**, 055708 (2013).
- [15] S. K. Sahu and P. Shanmugam, *Optics Express* **23**, 22291 (2015).
- [16] Y. Guo, Y. Wang, F. Jin and G. Li, *Water Tank Experiments for Laser Backward-Scattering Properties of Bubble Cluster*, IEEE/OES China Ocean Acoustics (COA), 2016.